42nd AIAA Aerospace Sciences Meeting and Exhibit
5 - 8 January 2004, Reno, Nevada

AIAA-2004-0878

Applications of Pressure-Sensitive Paint to Testing at Very Low Flow Speeds

James H. Bell*

ABSTRACT

Pressure-sensitive paints (PSP) might be a useful tool for studying low speed (V<30 m/s) flows. But the pressure field in these flows is characterized by small variations around a large mean value (typically one atmosphere). Since PSP brightness depends on absolute pressure level, small variations around a large mean pressure result in similarly small variations in PSP luminescence. To maximize signal-to-noise ratio, attention must be paid to both random error, primarily due to photon shot noise, and bias error due to brightness shifts induced by model temperature and position changes. In general, reduction of random error results in increased signal acquisition time, which increases bias error, and vice versa.

An experimental study in a small, low speed wind tunnel was designed to determine when reduction in bias error or random error is more desirable for improving overall PSP accuracy. A biluminophor PSP was used to provide a pressure-insensitive correction signal. Pressure-sensitive and pressure-insensitive luminescences were measured simultaneously with side-by-side cameras. Error levels of 22 Pa were obtained in pressure measurements on a small wind tunnel model, at a flow speed of 17 m/s (M=0.05). Results show that in a sufficiently well-controlled experiment, correction of data with a reference luminophor is unnecessary. However, the reference luminophor allows an important degree of operational flexibility.

NOMENCLATURE

A,B	PSP calibration coefficients with arbitrary pressure reference
b	Model span
c	Model chord
I	Paint luminescence intensity
k	PSP calibration coefficient with vacuum reference
M	Mach number
p	Pressure
V	Free-stream velocity
α	Angle of attack

Subscripts

v	Condition at vacuum
0	Reference condition (usually 1 atmosphere pressure)

Acronyms

PSP	Pressure-sensitive paint
RMS	Root-mean square
SNR	Signal-to-noise ratio

* Aerospace Engineer, NASA Ames Research Center, Member AIAA

INTRODUCTION

Pressure-sensitive paint (PSP) relies on the existence of luminescent materials whose light emission in response to illumination at some excitation frequency is dependent on the local air pressure. Further details of this phenomenon are well covered in several review papers[1,2,3]. To first order, the brightness of a PSP is sensitive to pressure in an inverse-linear sense, i.e., as

$$\frac{I}{I_v} = \frac{1}{1+kp} \tag{1}$$

where I is the light intensity emitted at pressure p, and k is a constant dependent on the paint chemistry. Typical values of k range from 1 to 6 atm^{-1}. A value of k=4 atm^{-1} approximates the PSP formulation used for the current experiment. Since I will naturally vary with other factors, such as paint thickness and excitation light intensity, it is necessary to normalize by a reference measurement – in this case the brightness I_v of the paint in a vacuum. In wind tunnel testing a vacuum reference is rarely available, and but a reference at an arbitrary pressure can easily be substituted through a slight modification of equation 1:

$$\frac{I_0}{I} = A + B\frac{p}{p_0} \tag{2}$$

Here I is again the light intensity emitted at pressure p, I_0 is the light intensity emitted at pressure p_0, and A and B are calibration coefficients which depend on k and p_0. A and B must sum to 1. (E.g., if k=4 atm^{-1} and p_0=1 atm, A=0.2 and B=0.8.) PSP brightness is also sensitive to temperature. A typical PSP might have a temperature

sensitivity of 0.5%/°C. Note that equation (2) assumes that PSP temperature and excitation intensity do not change between the acquisition of the test and reference data points. Any change would result in a bias error.

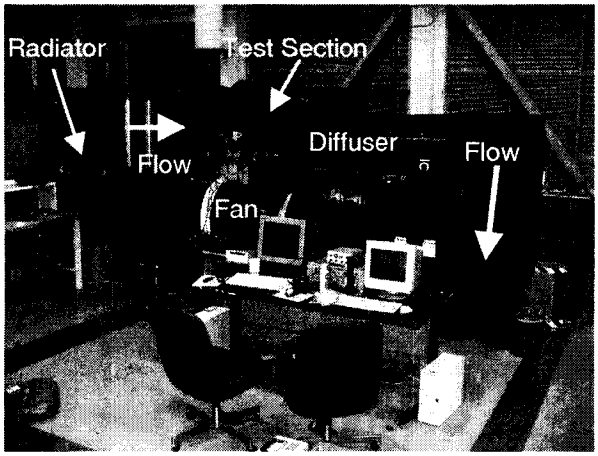

Figure 1. PSP Research Tunnel. Closed-return tunnel driven by 75 Kw electric fan. Flow temperature controlled by radiator.

The linear pressure-sensitivity of PSP limits its usefulness at low flow speeds, where the pressure changes of interest are small compared to the static pressure. For example, in a test at V=30 m/s, at a static pressure of 1 atm, the total range of pressure variation might be close to the dynamic pressure – about 550 Pa. Measurements with an accuracy of 20 Pa might be desirable to resolve surface pressure features. For the typical PSP cited above, a 20 Pa pressure change around 1 atm results in a brightness change of 0.024%. This puts stringent limitations on the allowable level of fluctuation in surface temperature as well as excitation lamp brightness. PSP camera accuracy is similarly constrained; the camera must measure light intensity with a signal to noise ratio greater than 4200:1. This requirement is significant, because the accuracy light intensity measurements are fundamentally limited by photon shot noise: the signal-to-noise level of any light intensity measurement cannot be greater than the square root of the number of photons collected to make the measurement. In scientific grade CCD cameras, shot noise is typically the largest component of random noise in the measurement, and single image shot noise SNRs of more than 500:1 are exceptional.

For a given PSP test setup, bias errors are reduced by acquiring the test and reference data points as rapidly as possible, thus minimizing the time available to temperature and lamp fluctuations. On the other hand, random error is primarily due to shot noise, which can be minimized by increasing the number of photons acquired, and thus data acquisition time. Ideally, the experimenter wishes to reduce the sum of random and bias error, and so the question arises as to what is the optimum allocation of data acquisition time. The current study attempts to both answer this question for a specific case, and thus demonstrate the usefulness of PSP at very low flow speeds, as well as to develop general procedures for optimizing PSP measurement accuracy.

EQUIPMENT AND EXPERIMENTAL PROCEDURE

I. Test Equipment

Wind Tunnel. The experiments described in this paper were performed in the PSP research wind tunnel at the NASA Ames Research Center. The PSP tunnel (shown in figure 1) is a small closed return wind tunnel, with the test section arranged vertically above the drive fan. The drive fan is powered by a 75 KW electric motor, which is located within the fan housing. The motor/fan unit rests on flexible mounts which isolate it from the rest of the wind tunnel structure to minimize vibration. The tunnel itself is built of fiberglass with a metal frame. A radiator installed upstream of the contraction section circulates refrigerated water to cool the flow.

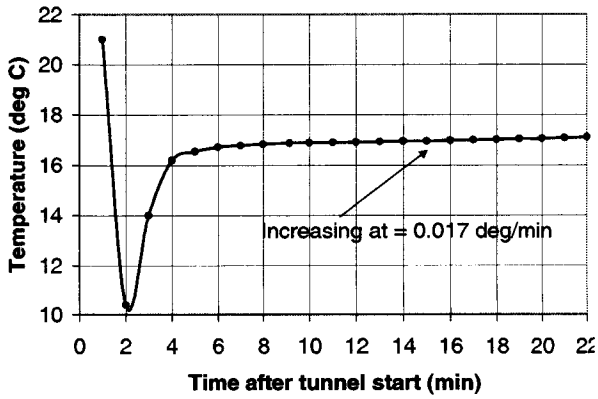

Figure 2. PSP tunnel settling chamber temperature. Motor started at time=0. Test section flow speed is 50 m/s

The PSP tunnel can be operated up to speeds of 120 m/s (M=0.35). However, at high speeds the heat rejection capacity of the cooling system is exceeded. If constant-temperature operations are desired, as in the present tests, the tunnel is limited to 60 m/s or below. The cooling system currently operates in an open loop control mode, so it is not possible to set a desired control temperature. Instead the tunnel must be operated with the cooling system on until its temperature stabilizes. A typical temperature history

curve is shown in figure 2. Initially the tunnel is at room temperature, 21° C, while the colling water reservoir has been pre-chilled to 3° C. When the tunnel starts, the flow initially cools rapidly but is thereafter heated by the motor. Whithin ten minutes, the flow approaches an equilibrium temperature. Note that the thermal mass of the tunnel is large enough that a true equilibrium is not reached. The heating rate simply falls to a low value (0.017° C/min under these conditions), which indicates the limit of temperature control capability for this facility.

The test section measures 30.5x30.5x61 cm. The sidewalls are made of UV-transparent plexiglas, while the top and bottom walls are aluminum. The top and bottom walls have cutouts for model-mounting hardware. All non-transparent parts of the test section are painted flat black to reduce extraneous reflections.

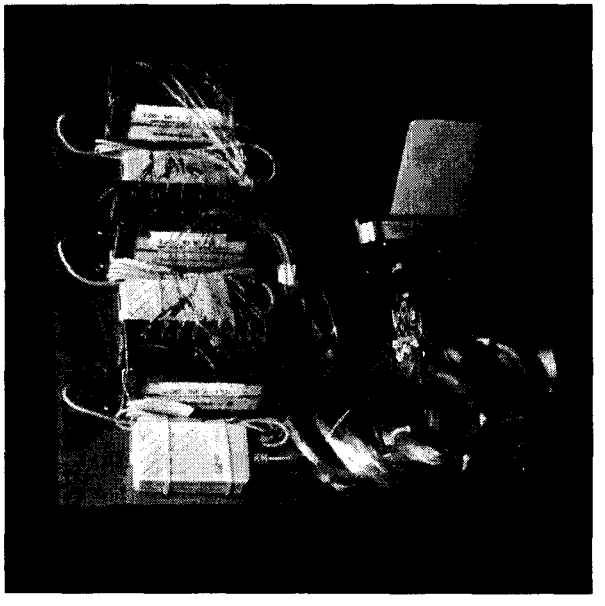

Figure 3. Photograph showing painted Lockman wing model in upper right hand corner as well as mounting hardware and connections to three conventional pressure arrays.

Model. The model used for these experiments is shown, along with its conventional pressure measurement system, in figure 3. The model is a 15.2 cm span, 10.2 cm chord, 20° swept wing with an NACA 0012 airfoil shape, originally built and tested by Lockman and Seigmiller[4]. It will be referred to in the text as the Lockman wing. The model is designed to be mounted so that it protrudes directly from a wind tunnel sidewall into the flow. The Lockman wing is equipped with 41 functional static pressure taps in three chordwise rows. Plastic tubing is used to connect these taps to three Scanivalve DSA 3017 digital sensor arrays with a pressure range of ±34 kPa (±5 psi) and a resolution of ±3 Pa (±0.004 psi).

PSP. For this test the suction surface of the Lockman wing was coated with type BF40-405 pressure-sensitive paint, supplied by Innovative Scientific Solutions, Inc. BF40-405 is a biluminophor paint. The pressure-sensitive luminophor emits light with a peak wavelength of 650 nm, while the reference luminophor emits with a peak wavelength of 545 nm. The relative luminophor concentrations are adjusted such that they have roughly the same brightness when viewed at a pressure of one atmosphere while being excited by light at 405nm. Most pressure-sensitive paints are intended to be used with a base coat or screen layer which covers the model and provides a optically uniform, chemically benign surface for the pressure-sensitive topcoat to adhere to. BF40-405 contains scattering agents that in allow it to be used without a base coat. However a base coat is preferred when, as in this case, time is available for its application. For the present test a urethane basecoat also manufactured by Innovative Scientific Solutions was first applied to the model. The basecoat was wet-sanded with 5 micron sandpaper to reduce the mean surface roughness from 0.6 microns to 0.24 microns. Brown[5] argues that by evening out the surface, sanding reduces variation in the reflectivity of the base coat. This reduces the spurious signal that would otherwise arise when images taken with the model in slightly different positions are ratioed.

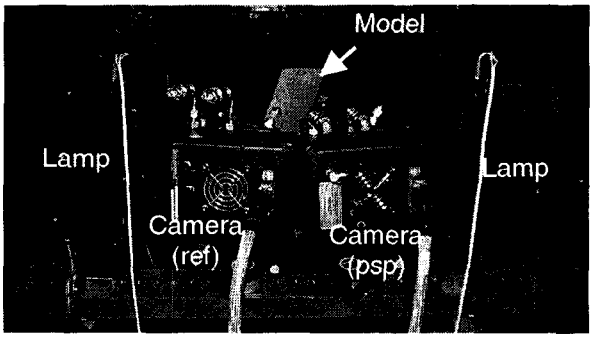

Figure 4. Close-up photo of test section showing LED lamps, cameras, and model visible through window in test section wall. Flow is left to right. Cameras and lamps are mounted on a rigid frame attached to test section structure.

Cameras. Figure 4 shows a close-up view of the model in the test section, viewed by two cameras and illuminated by two lamps. The cameras, built by Roper Scientific, use SITe 1024x1024 pixel back-illuminated, thermoelectrically cooled CCDs. The CCDs are read out at 900 KHz using the 14-bit ADC installed in the Roper Scientific ST-138 camera controller. Readout time is about 1.1 seconds per exposure. The SITe CCDs have a full-well capacity of 330,000 electrons/pixel, but

are normally operated below saturation. Typically exposure times are adjusted so that the average pixel collects about 250,000 photoelectrons during an exposure, resulting in a shot-noise SNR of 500:1. The SNR for readout noise, in contrast, is about 12,500:1 under the current conditions, so shot noise is the limiting noise source for these cameras. Both cameras were equipped with identical 50 mm lenses set to f2.8, and both were set to the same exposure time.

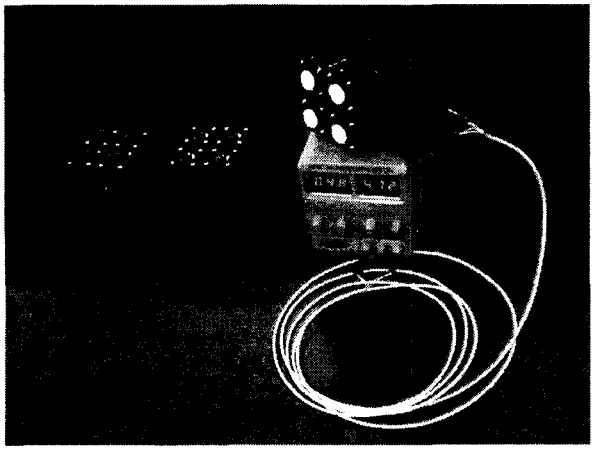

Figure 5. Custom-built lamp unit, showing four 405nm LED arrays operating and constant current power supply. Two more lamps are shown on left side (without power supplies).

Lamps. The lamps were custom-built at Ames Research Center, and are shown in more detail in figure 5. Each lamp is built around a set of four 405nm LED arrays. Each LED array has an integral reflector and using a blue short pass interference filter to minimize lamp output at the paint emission wavelengths. The array/reflector combinations were developed by Timothy Bencic of the NASA Glenn Research Center. The four arrays in each lamp are connected in series and driven by a constant current power supply. Illumination at 405 nm is convenient in that it efficiently excites most PSPs, but is not considered to be a UV safety hazard. (What hazard, if any, might arise from near-UV illumination is not well established, and some form of eye protection is still advisable.) The LED arrays, manufactured by Optotech, Inc., are an efficient and convenient means for generating near-UV light.

II. Data Reduction Procedures

All data reduction in this study begins with raw images, which are images taken of the model under a defined pressure condition with the camera's lens filtered to admit only light of the desired wavelength. Raw images taken with the tunnel running at the test condition are "wind-on" images. Those taken with the tunnel off are "wind-off" images. Images taken at the emission wavelength of the pressure-sensitive luminophor are "PSP" images. Those taken at the emission wavelength of the pressure-insensitive luminophor are "reference" images. (In the current test, one camera was normally used for PSP images and another for reference images.) Each raw image was the mean of several individual exposures of the camera. Averaging multiple exposures reduces photon shot noise while increasing data acquisition time. It is a convention at NASA Ames to choose some power of two for the number of exposures to be averaged to form an image.

Two corrections are applied to each raw image to reduce its noise level. To remove pixel-to-pixel variations in bias, a "dark" image is subtracted from each raw image. The dark image is just an image taken under exactly the same conditions as the raw image but with the camera shutter closed. In the absence of light, the signal read out from each pixel is that pixel's bias level. To remove pixel-to-pixel variations in gain, the raw image (after dark subtraction) is ratioed with a "flat field" image. This is an image taken of an evenly illuminated flat white surface. Since the surface brightness is the same across the image, differences in measured brightness between pixels represent differences in gain. Flat field images in this experiment were obtained by placing a pair of translucent opal glass filters back-to-back in front of the lens. (The flat field image must be dark-subtracted as well.)

While dark and flat field corrections reduce bias errors they increase random errors. Mendoza[6] points out that noise in the dark images adds to the overall image noise in an RMS fashion, while flat field noise adds to overall noise directly. Correction images were averaged until their shot-noise noise contribution was low compared to that of the raw images. The intensity levels in the dark images are low compared to those in the raw images, and so their noise contribution is also low. It was only necessary to average four or occasionally 16 exposures to reduce the dark image noise contribution sufficiently. Due to their higher intensity levels, flat field images have a much higher noise contribution, and it is desirable to average as many exposures as conditions will allow. In this study flat field images were formed from the mean of 512 individual exposures.

Dark and flat field corrected raw images were further reduced to obtain pressure data, using two different methods. In the single channel method, only PSP wavelength images are used. Following equation (2), it is desired to form the pixel-by-pixel ratio of the wind-on and wind-off images. However, the model or camera may shift due to airloads or vibration when the tunnel is turned on or off. Therefore the wind-on image must be "correlated" to match the wind-off image. This is done

by finding the locations of the dark target marks that are applied to the model. The target centers are located to sub-pixel accuracy using a centroid finder. The wind-on image is then warped with a biquadratic transform to line up the targets in both images, following the method outlined by Bell & McLachlan[7]. Once this is done the correlated wind-on image is used to divide the wind-off image on a pixel-by-pixel basis. Pixel intensities in the resulting "ratioed" image are linearly related to pressure following equation (2).

The single channel method is sensitive to errors due to any change in lamp brightness between the acquisition of wind-on and wind-off images, or due to model motion with respect to the lamps. These errors can be corrected using the biluminophor data reduction method. Reference images taken in the wavelength emitted by the paint's pressure-insensitive luminophor are used to detect variations in paint brightness due to model motion and lamp variation. In the current experiment, wind-on and wind-off images were taken with a separate camera filtered to detect only light emitted by the reference luminophor. The wind-on reference image was correlated to match the wind-off reference image with the same procedure used for the PSP images, and a second ratioed image was formed. This correction image was then used to normalize the PSP ratioed image. Since the reference and PSP images were taken by separate cameras, there must be some accounting for the difference in viewing angles. This was done by projecting both images onto a 3D surface grid of the Lockman wing. The texture-mapping method described by Bell & Schairer[8] was used to maintain the full resolution of the original 2D images. Biluminophor data reduction only partially corrects for errors due to temperature difference between the wind-on and wind-off images, since the temperature sensitivity of the reference luminophor is not identical to that of the pressure-sensing luminophor.

In the current test, intensity ratio values were converted to pressure values using *in situ* calibration. The pressure measured by each tap was compared to the PSP intensity ratio at the tap location. A first-order least squares fit was used to determine the coefficients of a linear equation relating intensity ratio to pressure. The accuracy of the PSP is then measured by the scatter between the tap and PSP results. The final result is referred to as the "calibrated" image.

RESULTS AND DISCUSSION

Initially, PSP data were obtained at a flow speed of V = 34 m/s, (M=0.1) for checkout purposes. Figure 6 shows a PSP image reduced using the single channel procedure. The image is false colored to show low pressure regions in blue, and high pressure regions in red. High-contrast marks on the wing, especially the taps and reference targets, are still visible in the image. The free-stream pressure is set to zero. The pressure distribution over the wing is characteristic of upper surface flows at low Reynolds numbers (in this case, chord Re = 230,000). A flat topped region of low pressure marks a separation bubble. As the flow reattaches there is a rapid recovery to the free-stream pressure. This behavior can also be clearly seen in figure 7, which shows a line cut through the image data along a chordwise line at midspan. (Image data were projected onto a 3D surface grid to determine the correct surface coordinates.)

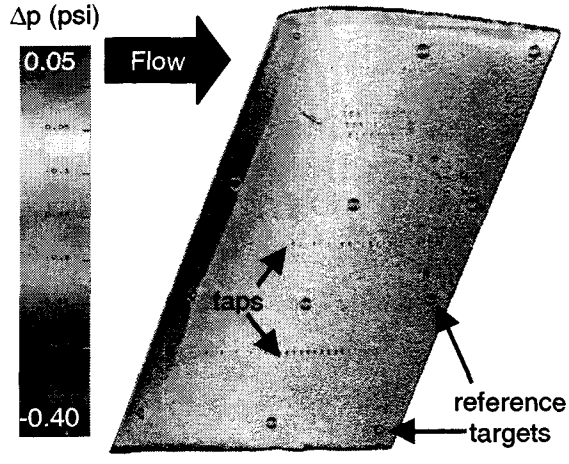

Figure 6. False-colored image showing pressure distribution over Lockman wing at V=34 m/s, α=6°. Taps and reference marks used in data reduction can also be seen in image.

A comparison between the tap and PSP data is shown in figure 8. The RMS difference between tap and PSP results is only 0.01 psi, which is 2.8% of the pressure variation over the wing. Data reduction using the biluminophor method (not plotted here) also gives an RMS scatter between paint and taps of 0.01 psi. This suggests that errors due to model motion and lamp variation are not significant. In fact, model motion from the wind-on to wind-off images is roughly 0.2 pixels, about 0.1 mm. The primary remaining uncorrected error source is temperature variation between the wind-on and wind-off images. Overall temperature measured in the settling chamber varied by 0.13° C between the two conditions. In this experiment, wind-on and wind-off images are the sum of 64 exposures.

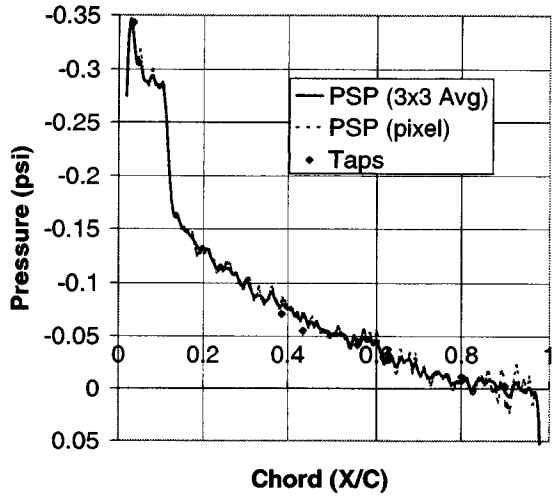

Figure 7. Line cut through midspan (y/b=0.5) of Lockman wing at condition corresponding to image data shown in figure 6. Cuts show results taken from individual pixels on a line and from a 3x3mean of adjacent pixels.

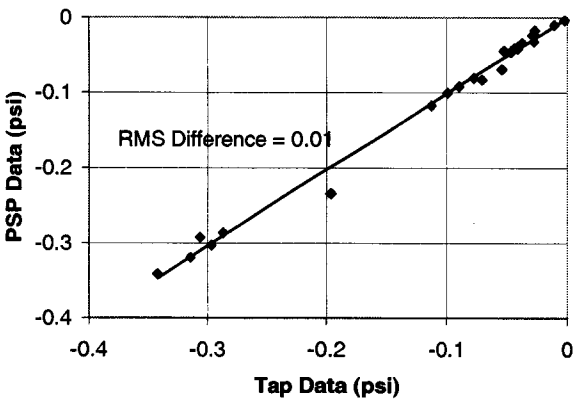

Figure 8. Scatter plot showing tap data *vs.* PSP data at tap locations for the image data shown in figure 6. RMS difference between the two data sources is 0.01 psi.

Further studies were all carried out at V = 17 m/s (M=0.05). Because the tunnel was run at lower speed model motion and temperature variation are lower than they were in the previous case. Model motion was roughly 0.02 pixels, or 0.01 mm, while no change in settling chamber temperature was detected. To further reduce the contribution of photon shot noise, images were formed from the sum of 128 exposures. A pressure image using single-channel data reduction is shown in figure 9. There is significant three-dimensionality in the pressure distribution relative to the higher speed case of figure 6. The scatter plot in figure 10 shows an RMS difference of 0.006 psi between the tap and PSP data. While lower in absolute terms than the higher speed case, the RMS difference of 0.006 psi is 10% of the overall pressure variation of 0.06 psi. This is much higher relative to the pressure range than the 2.8% variation found in the higher speed case. It suggests that the three-dimensionality seen in figure 9 is spurious.

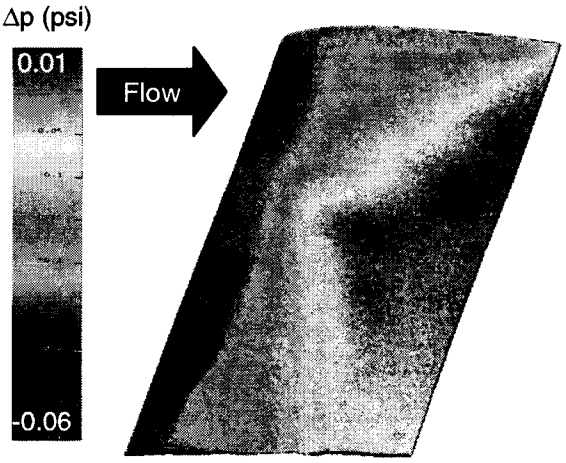

Figure 9. False-colored image showing pressure distribution over Lockman wing at V=17 m/s, α=6°. Data reduction uses only wind-on and wind-off images from pressure-sensitive luminophor in paint.

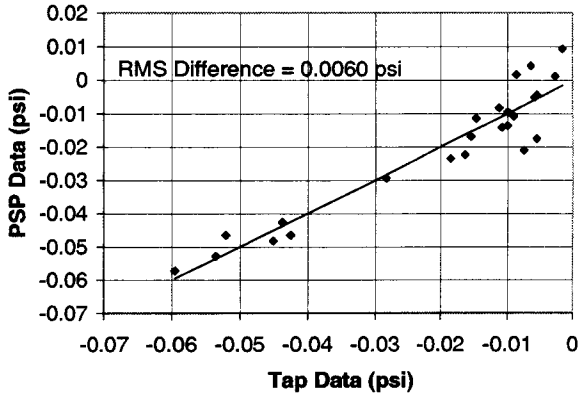

Figure 10. Scatter plot showing tap data *vs.* PSP data at tap locations for the image data shown in figure 9. RMS difference between the two data sources is 0.006 psi.

The small change in model position might suggest that there were few sources of bias error that the biluminophor technique could correct. However, biluminophor data reduction was still performed, with the result shown in figure 11. These data more closely resemble the two-dimensional pressure distribution of figure 6. The low pressure suction region extends over a somewhat greater chord length (18% of chord for fig 11 vs. 11% for figure 6) which is consistent with the reattachment line moving downstream as Reynolds number decreases. However the degree of random noise

in the data, as shown by the amount of perceived "graininess" in the image, has increased significantly. Random noise would be expected to about double due to the noise contribution of the reference images. In addition any alignment error in the photogrammetric correction will add noise.

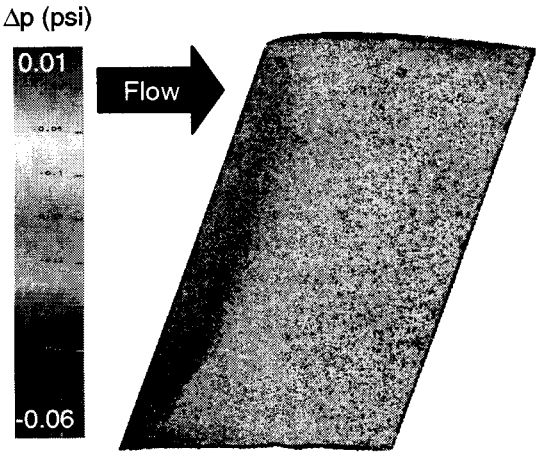

Figure 11. False-colored image showing pressure distribution over Lockman wing at V=17 m/s, α=6°. Data reduction uses biluminophor method. Note increase in image graininess (perceived noise) *vs.* figure 9.

Figure 12 shows the RMS difference between tap and PSP data for the case of figure 11. The RMS scatter is reduced compared to the single channel data reduction method of figures 9-10. The RMS scatter of 0.0046 is 7.7% of the pressure range, as opposed to 10% of the pressure range for the previous case.

However the single channel data reduction method still offers the advantage of lower random error, if bias error sources can be reduced. One approach is to run the wind tunnel in such a way as to minimize bias error. Fir this study, this was done by:

1. Running for an hour prior to wind-on data acquisition, to allow the tunnel to reach true thermal equilibrium followed by immediate shutdown and wind-off data acquisition.
2. Raw images formed from 64 exposures each, instead of 128, to trade off random noise for reduced data acquisition time.
3. A tunnel shutdown procedure designed to minimize vibration and thus model motion between wind-on and wind-off conditions.
4. Shutdown of the cooler immediately prior to tunnel shutdown. This reduces the thermal transient relative to shutting down the cooler immediately after shutdown

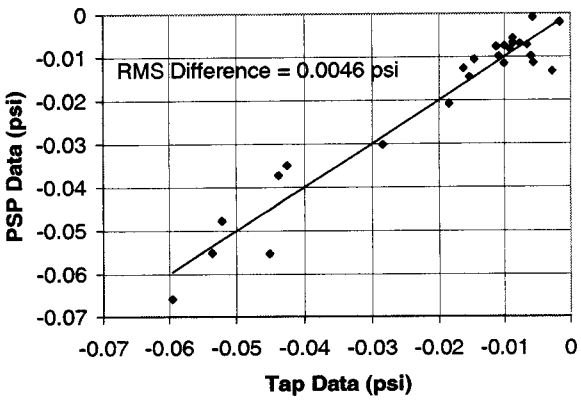

Figure 12. Scatter plot showing tap data *vs.* PSP data at tap locations for the image data shown in figure 11. RMS difference between the two data sources is 0.0046 psi.

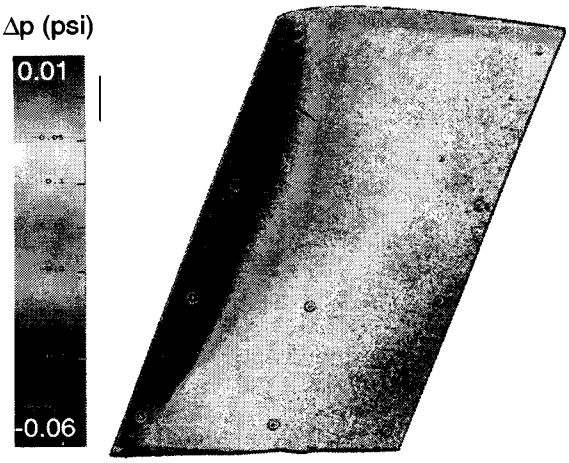

Figure 13. False-colored image showing pressure distribution over Lockman wing at V=17 m/s, α=6°. Data reduction uses only wind-on and wind-off images from pressure-sensitive luminophor in paint. Compare with figure 9 to see effect of more careful control of temperature drift between wind-on and wind-off measurements.

When these procedures were followed, the results shown in figure 13 were obtained. Indications of three-dimensionality are considerably reduced relative to figure 9, although there is still more apparent three-dimensionality than in figure 11. The scatter plot for this case (figure 14) shows an RMS difference between paint and taps of only 0.0033 psi, or 5.5% of the pressure range. A chordwise cut at midspan (figure 15) shows good agreement with pressure tap data, although the relative noise level is increased compared to the data in figure 7.

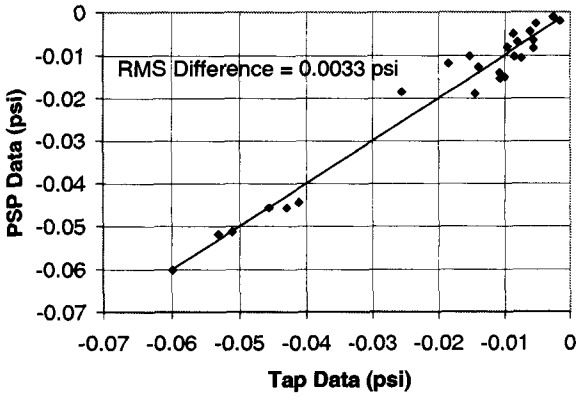

Figure 14. Scatter plot showing tap data *vs.* PSP data at tap locations for the image data shown in figure 13. RMS difference between the two data sources is 0.0033 psi.

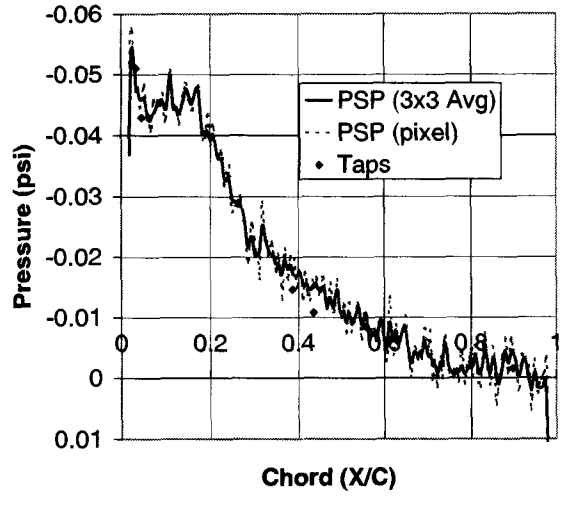

Figure 15. Line cut through midspan (y/b=0.5) of Lockman wing at condition corresponding to image data shown in figure 13. Cuts show results taken from individual pixels on a line and from a 3x3mean of adjacent pixels.

CONCLUDING REMARKS

Careful experimental technique and the use of biluminophor paints and data reduction can extend the useful range of PSP down to very low flow speeds compared to the transonic regime in which PSP was initially developed. PSP error levels of .0046 psi and .0033 psi can be obtained via biluminophor and single channel data reduction, respectively, at a flow speed of 17 m/s, where the entire range of observed pressure variation is only 0.06 psi.

While careful control of tunnel temperature and shutdown procedures yields superior results with single channel data reduction, these may not be generalizable to all experiments of interest at low speeds. In many cases, it may not be possible to run the tunnel until it reaches thermal equilibrium, or to employ an extremely rigid model. In these cases, bias errors in single channel data reduction will be unacceptably high, and the only recourse will be to use the biluminophor method, despite its higher random error.

[1] Liu T, Campbell B, Burns SP, Sullivan JP, Temperature- and Pressure - Sensitive Paints in Aerodynamics, 1997 *Applied Mechanics Rev.*, vol 50, no. 4, 01-Apr-97

[2] Bell JH, Schairer ET, Hand LA, Mehta RD. 2001 Surface Pressure Measurements Using Luminescent Coatings. In *Ann. Rev. Fluid Mech., vol. 33, pp.* 155-206.

[3] Bell JH, Bencic T. 2003 Optical Metrology for Fluids, Combustion, and Solids Chapter 12: Luminescent Paints for Pressure and Temperature Measurements *Kulwer Academic, NY*

[4] Lockman, W.K. & Seegmiller, H.L. 1983 An Experimental Investigation of the Subcritical and Supercritical Flow About a Swept Semispan Wing, NASA TM 84367, June

[5] Brown, O., 2000 Low-Speed Pressure Measurements Using a Luminescent Coating System, PhD Thesis, Stanford University, May

[6] Mendoza, D.R. 1997 Limiting Mach Number for Quantitative Pressure-Sensitive Paint Measurements *AIAA Journal, Vol. 35, No. 7 pp. 1240-1241*

[7] Bell, J.H., McLachlan, B. 1996 Image Registration for Pressure Sensitive Paint Applications *Experiments in Fluids Vol. 22, pp. 78-86*

[8] Bell, J.H. and Schairer, E.T. 2002 Texture Mapping for Display and Analysis of Image Data on 3D Surfaces. , *AIAA Paper 2002-0745,* 40th Aerospace Sciences Meeting, Reno, Nevada, January 14-17.